

## 8 Surface structure and electronic state

### – Surface studies by using total-reflection high-energy positron diffraction (TRHEPD) and other methods –

*Project Leader: Ken Wada*

#### 8-1 Introduction

Surface and near-surface structures have large effects on the properties of industrial materials, especially those used for nanoelectronics devices and as catalysts. To develop those materials efficiently, definitive knowledge of the material surface and near-surface structures is essential.

Recently, it has been revealed that reflection high-energy positron diffraction (RHEPD), a positron counterpart of reflection high-energy electron diffraction (RHEED), is an ideal method for solid surface and near surface structure analysis. In contrast to the electron, the positron is totally reflected from the material surface when the glancing angle is smaller than a certain critical angle because of the positive crystal potential energy for the positron (Fig. 1). In the total reflection condition (e.g.,  $< 2^\circ$  for Si with 10-keV positrons, which is wide enough for the typical observation angle range of  $< 6^\circ$ ), the positrons are reflected from the topmost surface. This method also gives information on the near surface structure without background signals from the deeper atoms when the glancing angle is larger than the critical one. Emphasizing the advantage of using total reflection, we propose renaming the RHEPD method as total-reflection high-energy positron diffraction (TRHEPD).

We have started a project “Surface structure and electronic state”, which makes use of TRHEPD for surface structure analysis and other complementary methods for determining surface electronic states, e.g. angle-resolved photoemission spectroscopy (ARPES), to obtain full information at and near the surface.

We report briefly the TRHEPD experiment station at the KEK Slow Positron Facility (SPF) and present the results of determining the structure of

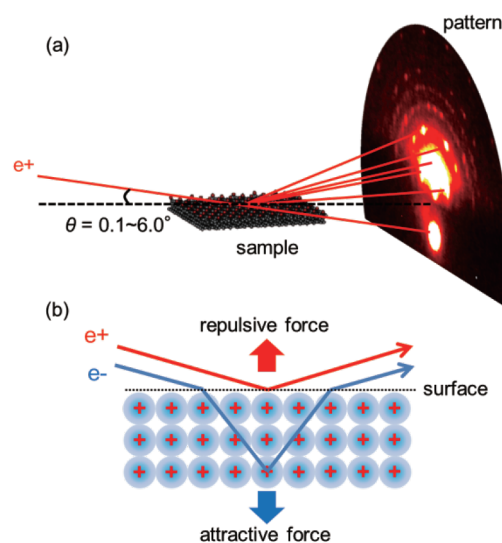


**Fig. 1:** (a) Experimental setup of RHEPD and (b) schematics of positron and electron beam incidences on crystal surface.

silicene on a Ag(111) surface performed in fiscal 2013 together with that of the structure of Pt-induced nanowires on Ge(001) in the preceding fiscal year as the first report on this project.

#### 8-2 TRHEPD experiment station at KEK-SPF [1,2]

First proposed by Ichimiya in 1992 [3], TRHEPD uses positrons of approximately 10 keV in energy and directs them at a crystal surface with a glancing angle smaller than typically  $6^\circ$ . The usefulness of this technique was proved by Kawasuso and Okada [4] in 1998 at JAEA, Takasaki, with an apparatus using a  $^{22}\text{Na}$  positron source providing a beam of  $10^3 \sim 10^4$  slow- $e^+$ /s. This apparatus was subsequently modified [5] and yielded fruitful results in determining the structures of metal-deposited surfaces of Si and Ge crystals [6], some

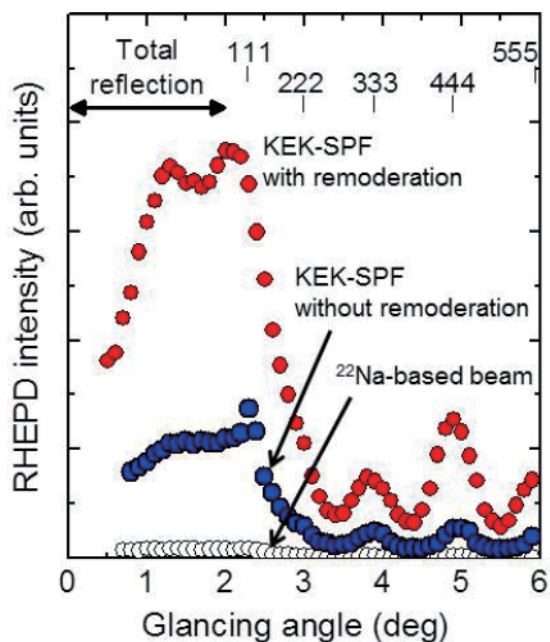


**Fig. 2:** RHEPD rocking-curves from a Si(111)-(7×7) surface observed with 10-keV positron beams [2]. The data obtained by the linac-based beams with and without remoderation at KEK-IMSS-SPF, and that by a  $^{22}\text{Na}$ -based beam are presented.

of which were impossible or very difficult to characterize by other techniques.

In 2010, the TRHEPD station was moved to the Slow Positron Facility (SPF) at KEK, where an intense slow-positron beam is produced using a dedicated linac (55 MeV, 600 W) and a production unit consisting of a Ta target (positron converter) and a W foil moderator. A high-intensity linac-based positron beam with an energy of 15 keV has been remoderated to be a 10-keV brightness-enhanced beam for TRHEPD experiments. This remoderation system has achieved a brightness enhancement of 1000-2000 times from the magnetically guided beam to the final low-emittance beam since 2012. The intensity of the specular spot from a Si(111)-(7×7) reconstructed surface observed by the present beam was found to be about 60 times higher than that observed by using the previous  $^{22}\text{Na}$ -based system (Fig. 2). An improved signal-to-noise ratio in the diffraction pattern due to the intensified beam flux allowed clear observation of fractional-order spots in the higher Laue zones, which had not been observed previously. With this linac-based system, it is shown that the RHEPD pattern from a Si(111)-(7×7) reconstructed surface for the total reflection condition, that is, the total-reflection high-energy positron diffraction (TRHEPD) pattern, does not contain contributions from atoms in the bulk.

### 8-3 Silicone on a Ag(111) surface [7]

Silicene, which is a two-dimensional atomic sheet composed of silicon, an analog of graphene, is attracting much attention as a possible material for next-generation electronic devices. In 2012, synthesis of silicone on a Ag(111) surface was successfully performed [8,9]. Silicene has also been formed on an iridium surface and a zirconium diboride thin film grown on a Si(111) surface [10,11].

The two-dimensional symmetry of silicene on a Ag(111) surface, predicted by theoretical calculations, was verified by scanning tunneling microscopy observations [12,13]. However, a buckled structure due to the strong  $sp^3$ -bonding character predicted by the theories [12,13], as shown in Fig. 3, had not been confirmed. The buckling feature is in sharp contrast to the case of graphene, which is a flat sheet. The calculated shape of the Dirac cone of the energy dispersion in silicene is modulated by the magnitude of buckling in the silicene sheet [14] as well as by interactions with the Ag(111) surface [15]. Thus, the gap between the top and the bottom Si layers in silicene and that between the bottom Si and the top Ag layers are important factors in understanding its electronic properties.

To determine the detailed structure, first the positron beam was injected at  $13^\circ$  off the  $[11\bar{2}]$  direction (one-beam condition). Such an off-symmetry positron direction causes the specular

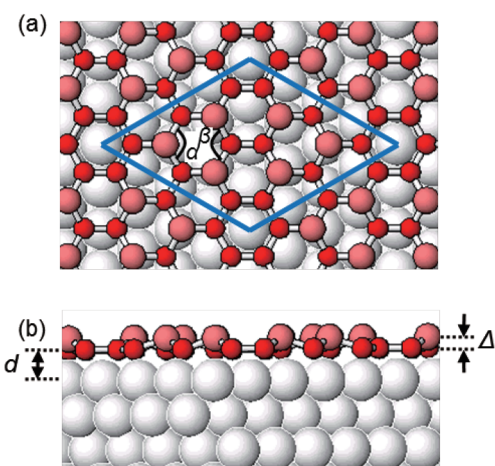


**Fig. 3:** Structure of silicone on a Ag(111) surface ((a): top view and (b): side view) [7]. Light and deep red circles indicate the upper and lower Si atoms in silicone, respectively. Gray circles indicate the Ag atoms. The gap between the upper and lower Si layers and that between the lower Si and the first Ag layers are denoted by  $\Delta$  and  $d$ , respectively. The bond angles of Si in silicone are denoted by  $\alpha$  and  $\beta$ .

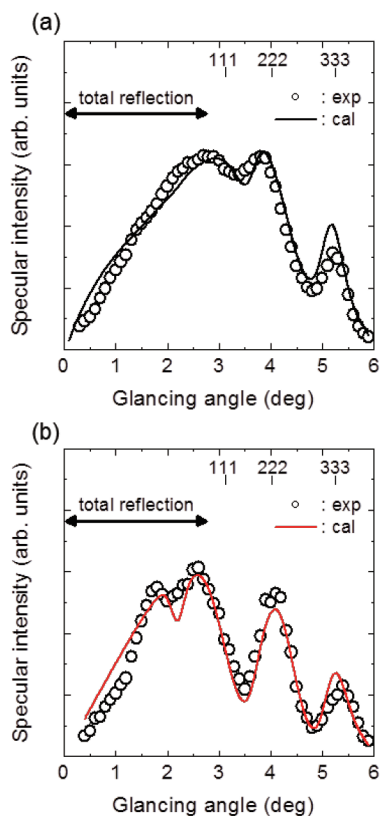


**Fig. 4:** TRHEPD rocking-curves for (a) the Ag(111) surface and (b) the silicene on the Ag(111) surface with the one-beam condition (the azimuth is  $13^\circ$  off from the  $[11\bar{2}]$  direction) at room temperature [7]. Open circles indicate the experimental data and solid lines show the curves calculated with the optimum parameters.

spot intensity to depend mainly on the vertical components of the atomic positions and the number density of atoms in each layer. This is because atoms in each layer are randomly distributed in each plane when viewed with a small glancing angle along this off-symmetry direction. By analyzing the specular spot intensity dependence of the beam glancing angle, which is called rocking-curve analysis, the vertical features of the structure were determined with the one-beam condition (Fig. 4) to be  $d = 2.14 \text{ \AA}$  and  $\Delta = 0.83$ . Then, the beam was injected along the exact  $[11\bar{2}]$  direction (many-beam condition), where each spot intensity depends on the in-plane atomic positions, as well as the vertical components. The in-plane positions were extracted by rocking-curve analysis for the specular spot with the many-beam condition (Fig. 5), with the fixed vertical values already known, to be  $\alpha = 112^\circ$  and  $\beta = 119^\circ$ . Table 1 summarizes these results with previous theoretical ones.

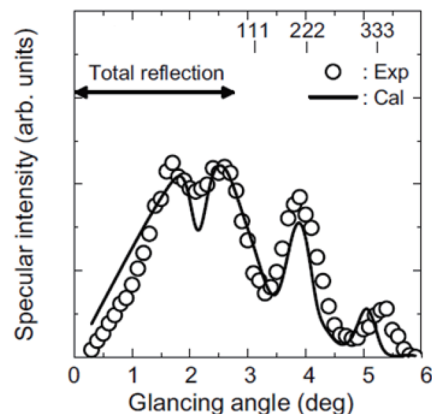


**Fig. 5:** TRHEPD rocking-curve for the silicene on a Ag(111) surface under the many-beam condition (The azimuth is along the  $[11\bar{2}]$  direction) at room temperature [7]. Open circles indicate the experimental data and solid line shows the curve calculated with the optimum parameters.

**Table 1:** Structure parameters determined for silicene on a Ag(111) surface by TRHEPD, and those from previous theoretical works [7].

	$\Delta$ (Å)	$d$ (Å)	$\alpha$ (°)	$\beta$ (°)
RHEPD*	0.83	2.14	112	119
Theory <sup>1</sup>	0.78	2.17	110	118
Theory <sup>2</sup>	0.7			

<sup>1</sup> Vogt *et al.*, Phys. Rev. Lett. **108**, 155501 (2012).  
<sup>2</sup> Lin *et al.*, Appl. Phys. Express **5**, 045802 (2012).

#### 8-4 Pt-induced nanowires on Ge(001) surface [16]

Self-assembled nanowires formed on semiconducting crystal surfaces have attracted a great deal of interest as they can further our fundamental understanding of one-dimensional (1D) properties such as the non-Fermi liquid and the Peierls-type metal-insulator transition [17]. Accordingly, extensive studies have been performed on surface 1D systems such as In/Si(111) [18-20], Au/Si(553),(557) [21], Y/Si(001) [22], Au/Ge(001) [23], and so on.

Recently, it was found that well-ordered and defectless nanowires are formed on Ge(001) surfaces by depositing a submonolayer of Pt atoms [24]. Three models have been proposed for this surface and near-surface structures. One is called the “Pt dimer (PD)” model, as shown in Fig. 6(a). In this model, the first surface layer is covered by Pt dimers on a  $\beta$  terrace [24,25] giving rise to a  $p(4 \times 2)$  unit cell. The  $\beta$  terrace is composed of alternating Ge-Ge and Pt-Ge dimers along nanowires. On the basis of the results of recent research on theoretical calculations, two models have been proposed for the Pt-induced nanowires [26,27]. Stekolnikov *et al.*

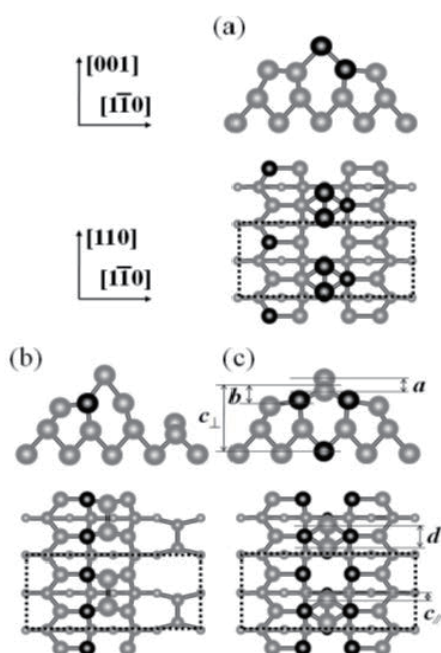


**Fig. 6:** Schematic illustrations of Ge(001)-p(4×2)-Pt; (a) PD, (b) TDC and (c) NW models [16]. The black and gray spheres represent Pt and Ge atoms, respectively. The dotted rectangles represent (4×2) unit cells. The interlayer and interatomic distances are labeled by  $a$ ,  $b$ ,  $c_{||}$ ,  $c_{\perp}$ , and  $d$ .

[27,28] suggested the tetramer-dimer-chain (TDC) model as shown in Fig. 6(b). In this model, the topmost layer is covered by Ge dimers and Pt atoms are placed in the second layer. The reconstructed p(4×2) unit cell contains 0.25 monolayers (ML) of Pt atoms. Figure 6(c) shows the nanowire (NW) model proposed by Vanpoucke et al. [26,29] In this model, the total coverage of Pt atoms is 0.75 ML and the surface periodicity is p(4×2). The two Pt arrays in the second layer are bridged by the top Ge dimers. Pt atoms are also placed in the fourth layer.

Despite extensive studies using scanning tunneling microscopy/spectroscopy (STM/S) and *ab initio* calculations, the atomic configuration and the phase transition mechanism of Pt-induced nanowires on Ge(001) surfaces have not been fully elucidated. There are only a limited number of diffraction and photoemission studies for this surface. In this study, we investigated a highly ordered Pt-induced nanowire on the Ge(001) surface using TRHEPD, and angle-resolved photoemission spectroscopy (ARPES).

To distinguish the correct one among the three models, we first performed TRHEPD rocking-curve analysis on the one-beam condition. Open circles in Fig. 7(a) show the rocking-curve for that condition at room temperature. Calculated rocking-curves

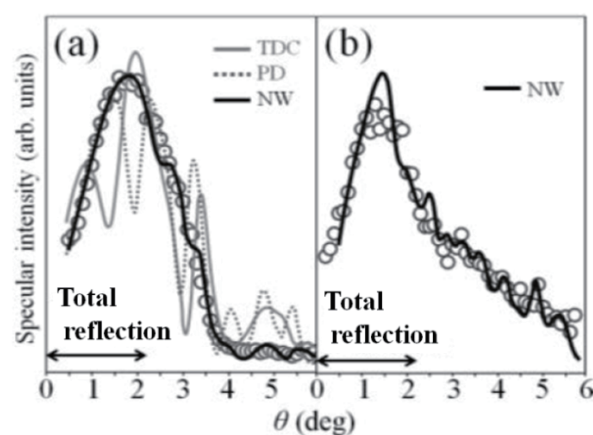


**Fig. 7:** TRHEPD rocking-curves on (a) one-beam condition, and (b) many-beam condition [16]. The open circles denote experimental data. The solid gray, broken gray, and solid black lines are the calculated curves for the TDC, PD, and NW models, respectively.

based on the three models, PD model (Fig. 6(a)), TDC model (Fig. 6(b)), and NW model (Fig. 6(c)), are shown by the broken gray, solid gray, and solid black lines, respectively. The NW model agrees well with the experimental result by adjusting Z-positions for the atoms. We have checked that more than ten other models proposed also disagree with the experimental result, and have determined that the NW model is correct, where the topmost atoms constituting nano wires are actually not Pt but Ge dimers. Next, we performed the rocking-curve analysis for the many-beam condition (Fig. 7(b)) and determined the three-dimensional atomic configuration of the system.

It is known that the p(4×2) periodicity of this surface at room temperature turns to be p(4×4) periodicity at low temperature [30]. To investigate the details of this phase transition, the rocking-curve analysis was performed at low temperature. Figure 8 shows rocking-curves for  $\theta = 1^\circ$  to  $4^\circ$  at room temperature (gray open circles) and 35 K (black open circles), indicating a displacive phase transition associated with a structure change. Based on the analysis at room temperature, possible p(4×4) periodicity structures were searched by displacing the atom positions with fixed atomic density. It was revealed that an asymmetric structure where two Ge dimers along with the wires are alternately inclined explains well the p(4×4) periodicity (black line in Fig. 8). It is a displacive phase transition originated from the change of Ge dimers structure from an asymmetric to a symmetric one. Table 2 lists experimental (present) and theoretical [29] interlayer and

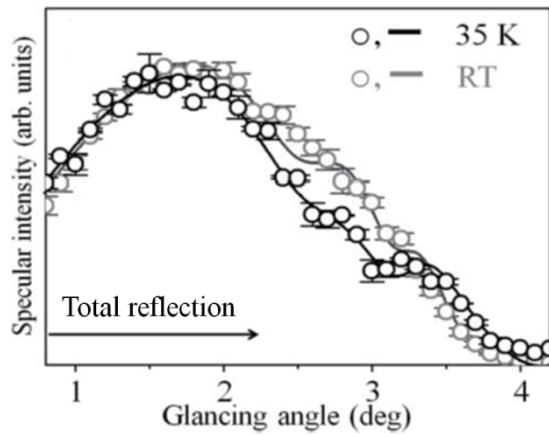


**Fig. 8:** Comparison of the experimentally obtained one-beam TRHEPD rocking-curves at room temperature (gray open circles) and 35 K (black open circles) [16]. The solid lines are the calculated curves based on the NW model.

**Table 2:** Interlayer and interatomic distances in the Pt-induced nanowire, as determined from the TRHEPD rocking-curve analysis [16]. The labels *a*, *b*, *c*, and *d* are denoted in Fig. 6(c). Theoretical values [29] are also listed.

	<i>a</i> (Å)	<i>b</i> (Å)	<i>c</i> (Å)	<i>d</i> (Å)
Low temperature	0.22 (±0.10)	0.74 (±0.17)	3.4 (±0.2)	2.9 (±0.2)
High temperature	0.04 (±0.09)	0.64 (±0.15)	3.3 (±0.2)	2.9 (±0.2)
Theory	< 0.03	0.52	3.13	2.72

interatomic distances of *a*, *b*, *c*, and *d* denoted in Fig. 6(c).

Figure 9(a) shows a typical low-energy electron diffraction (LEED) pattern from the Pt-induced vicinal substrate at room temperature. A double periodicity appears in the [110] direction with little sign of quadruple spots, whereas a quadruple periodicity prevails in the  $\bar{[110]}$  direction. These features suggest that most Pt-induced nanowires are aligned in the [110] direction. Thus, the Brillouin zones on the vicinal Pt/Ge(001) surface are single domains with a periodicity of  $p(4 \times 2)$ , as shown by solid rectangles in Fig. 9(b).

Figures 9(c) and 9(d) show the ARPES images taken along the [110] direction at 65 K and room temperature, respectively. In both images, the Ge bulk band appears at the center of the first surface Brillouin zone near the Fermi level, with parabolic dispersion toward the wave vector ( $k$ )  $\sim 0.2 \text{ \AA}^{-1}$  and binding energy ( $E$ ) of  $\sim 0.5 \text{ eV}$ . Another bulk band dispersion is seen from  $(k, E) \approx (0.1 \text{ \AA}^{-1}, 0.1 \text{ eV})$  to  $(k, E) \approx (0.4 \text{ \AA}^{-1}, 0.8 \text{ eV})$ . The dispersions around the  $\bar{J}$  point within the bulk band gap, as depicted in

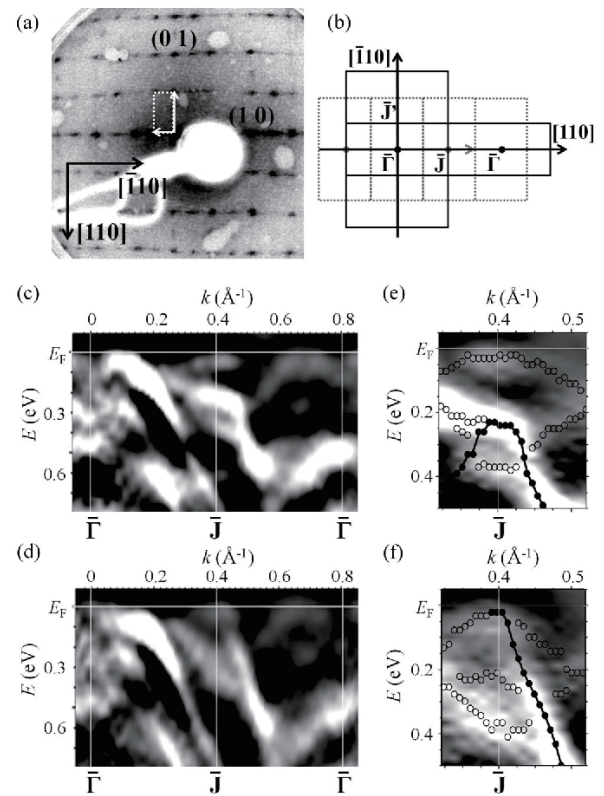


**Fig. 9:** (a) A LEED pattern from the Pt-induced nanowires on the vicinal Ge(001) substrate at room temperature. The energy of the incident beam is 80 eV. The dashed rectangle indicates the reciprocal unit cell. (b) The surface Brillouin zone of the  $p(4 \times 2)$  unit cell. The solid and dashed lines represent the orthogonally rotated domains. (c) and (d) Second derivatives of ARPES spectra obtained at 65 K and room temperature, respectively. The photoemission intensity is greater in the brighter areas in gray scale. The white vertical lines denote the  $\bar{\Gamma}$  and  $\bar{J}$  points. (e) and (f) Enlarged views of the areas around the  $\bar{J}$  point in (c) and (d), respectively. The solid and open circles represent the peak positions.  $E_F$  denotes the Fermi level. All figures are cited from [16].

Figs. 9(e) and 9(f), are attributed to the surface state bands. There are separable peaks denoted by open and solid circles by the peak-fitting procedure. The dispersions denoted by open circles are nearly the same at 65 K and room temperature. Unfortunately, the origins of these bands are not known at present. One possible explanation is the overlapping of the components of orthogonal minority domains. Theoretical calculation of the band structure based on the structure determined by TRHEPD is needed for further concrete discussion.

Temperature dependence of the specular spot intensity for the one-beam condition at  $\theta = 2.5^\circ$  in the temperature range 50–200 K was observed. The intensity gradually increases from 80 to 110 K

indicating the progress of the phase transition, and thereafter, a conventional Debye-Waller-like temperature dependence is observed within experimental error. From the slopes of the temperature-dependent specular intensity curve, the surface Debye temperatures are determined to be  $210 \pm 80$  K for the low-temperature  $p(4 \times 4)$  phase and  $130 \pm 40$  K for the high-temperature  $p(4 \times 2)$  phase.

#### References

- [1] K. Wada, T. Hyodo, A. Yagishita, M. Ikeda, S. Ohsawa, T. Shidara, K. Michishio, T. Tachibana, Y. Nagashima, Y. Fukaya, M. Maekawa, and A. Kawasuso, *Eur. Phys. J. D* **66**, 37 (2012).
- [2] K. Wada, T. Hyodo, T. Kosuge, Y. Saito, M. Ikeda, S. Ohsawa, T. Shidara, K. Michishio, T. Tachibana, H. Terabe, R. H. Suzuki, Y. Nagashima, Y. Fukaya, M. Maekawa, I. Mochizuki, and A. Kawasuso, *J. Phys.: Conf. Ser.* **443**, 012082 (2013).
- [3] A. Ichimiya, *Solid State Phenom.* **28-29**, 143 (1992).
- [4] A. Kawasuso and S. Okada, *Phys. Rev. Lett.* **81**, 2695 (1998).
- [5] A. Kawasuso, T. Ishimoto, M. Maekawa, Y. Fukaya, K. Hayashi, and A. Ichimiya, *Rev. Sci. Instrum.* **75**, 4585 (2004).
- [6] Y. Fukaya, M. Maekawa, I. Mochizuki, K. Wada, T. Hyodo, and A. Kawasuso, *J. Phys.: Conf. Ser.* **443**, 012068 (2013).
- [7] Y. Fukaya, I. Mochizuki, M. Maekawa, K. Wada, T. Hyodo, I. Matsuda, and A. Kawasuso, *Phys. Rev. B* **88**, 205413 (2013).
- [8] K. Takeda and K. Shiraiishi, *Phys. Rev. B* **50**, 14916 (1994)
- [9] M. Ezawa, *Phys. Rev. Lett.* **109**, 055502 (2012).
- [10] A. Fleurence, R. Friedlein, T. Ozaki, H. Kawai, Y. Wang, and Y. Yamada-Takamura, *Phys. Rev. Lett.* **108**, 245501 (2012).
- [11] L. Meng, Y. Wang, L. Zhang, S. Du, R. Wu, L. Li, Y. Zhang, G. Li, H. Zhou, W. A. Hofer, and H.-J. Gao, *Nano Lett.* **13**, 685 (2013)
- [12] P. Vogt, P. De Padova, C. Quaresima, J. Avila, E. Frantzeskakis, M. C. Asensio, A. Resta, B. Ealet, and G. Le Lay, *Phys. Rev. Lett.* **108**, 155501 (2012).
- [13] C.-L. Lin, R. Arafune, K. Kawahara, N. Tsukahara, E. Minamitani, Y. Kim, N. Takagi, and M. Kawai, *Appl. Phys. Express* **5**, 045802 (2012).
- [14] S. Cahangirov, M. Topsakal, E. Aktürk, H. Sahin, and S. Ciraci, *Phys. Rev. Lett.* **102**, 236804 (2009).
- [15] C.-L. Lin, R. Arafune, K. Kawahara, M. Kanno, N. Tsukahara, E. Minamitani, Y. Kim, M. Kawai, and N. Takagi, *Phys. Rev. Lett.* **110**, 076801 (2013).
- [16] I. Mochizuki, Y. Fukaya, A. Kawasuso, K. Yaji, A. Harasawa, I. Matsuda, K. Wada, and T. Hyodo, *Phys. Rev. B* **85**, 245438 (2012).
- [17] P. C. Snijders and H. H. Weitering, *Rev. Mod. Phys.* **82**, 307 (2010).
- [18] J. R. Ahn, J. H. Byun, J. K. Kim, and H. W. Yeom, *Phys. Rev. B* **75**, 033313 (2007).
- [19] C. González, Jiandong Guo, J. Ortega, F. Flores, and H. H. Weitering, *Phys. Rev. Lett.* **102**, 115501 (2009).
- [20] S. Hatta, Y. Ohtsubo, T. Aruga, S. Miyamoto, H. Okuyama, H. Tajiri, and O. Sakata, *Phys. Rev. B* **84**, 245321 (2011).
- [21] J. N. Crain and F. J. Himpsel, *Appl. Phys. A* **82**, 431 (2006).
- [22] C. Blumenstain, J. Schäfer, S. Mietke, S. Meyer, A. Dollinger, M. Lochner, X. Y. Cui, L. Patthey, R. Matzdorf, and R. Claessen, *Nature Phys.* **7**, 776 (2011).
- [23] Changgan Zeng, P. R. C. Kent, Tae-Hwan. Kim, An-Ping Li, and Hanno H. Weitering, *Nature Mat.* **7**, 539 (2008).
- [24] O. Gürłu, O. A. O. Adam, H. J. W. Zandvliet, and B. Poelsema, *Appl. Phys. Lett.* **83**, 4610 (2003).
- [25] D. E. P. Vanpoucke and G. Brocks, *Phys. Rev. B* **81**, 235434 (2010).
- [26] D. E. P. Vanpoucke and G. Brocks, *Phys. Rev. B* **77**, 241308(R) (2008).
- [27] A. A. Stekolnikov, F. Bechstedt, M. Wisniewski, J. Schäfer, and R. Claessen, *Phys. Rev. Lett.* **100**, 196101 (2008).
- [28] A. A. Stekolnikov, J. Furthmüller, and F. Bechstedt, *Phys. Rev. B* **78**, 155434 (2008).
- [29] D. E. P. Vanpoucke and G. Brocks, *Phys. Rev. B* **81**, 085410 (2010).
- [30] A. van Houselt et al., *Surf. Sci.* **602**, 1731 (2008).